

(NASA-CR-164759) GENERALIZED DUFORT-FRANKEL  
SPECTRAL METHODS Final Report, 1 Jun. 1980  
- 31 Aug. 1981 (Old Dominion Univ., Norfolk,  
Va.) 18 p HC A02/MF A01 CSCI 12A

881-32917

Unclas  
G3/64 27464

DEPARTMENT OF MATHEMATICAL SCIENCES  
SCHOOL OF SCIENCES AND HEALTH PROFESSIONS  
OLD DOMINION UNIVERSITY  
NORFOLK, VIRGINIA

GENERALIZED DUFORT-FRANKEL  
SPECTRAL METHODS

*By*

Liviu Lustman

Principal Investigator: William D. Lakin

Final Report  
For the period June 1, 1980 - August 31, 1981



*Prepared for the*  
National Aeronautics and Space Administration  
Langley Research Center  
Hampton, Virginia 23665

*Under*

Research Grant NAG-1-25  
Julius E. Harris, Technical Monitor  
High Speed Aerodynamics Division

May 1981

DEPARTMENT OF MATHEMATICAL SCIENCES  
SCHOOL OF SCIENCES AND HEALTH PROFESSIONS  
OLD DOMINION UNIVERSITY  
NORFOLK, VIRGINIA

GENERALIZED DUFORT-FRANKEL  
SPECTRAL METHODS

*By*

Liviu Lustman

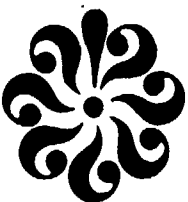
Principal Investigator: William D. Lakin

Final Report  
For the period June 1, 1980 - August 31, 1981

*Prepared for the*  
National Aeronautics and Space Administration  
Langley Research Center  
Hampton, Virginia 23665

*Under*  
Research Grant NAG-1-25  
Julius E. Harris, Technical Monitor  
High Speed Aerodynamics Division

*Submitted by the*  
Old Dominion University Research Foundation  
P.O. Box 6369  
Norfolk, Virginia 23508



May 1981

## TABLE OF CONTENTS

	<u>Page</u>
ABSTRACT . . . . .	1
GENERALIZED DUFORT-FRANKEL SCHEMES . . . . .	1
DIFFUSION EQUATIONS WITH CONSTANT COEFFICIENTS . . . . .	5
CONVECTION-DIFFUSION PROBLEMS . . . . .	6
BURGERS EQUATION . . . . .	8
DISCUSSION . . . . .	9
CONCLUSIONS . . . . .	10
REFERENCES . . . . .	11

## LIST OF FIGURES

### Figure

1	Divergence of Bénard problem at $Pe = 50$ showing lines of constant $\phi$ at $t = 4$ , computed using nine modes ( $T_0$ to $T_8$ ), $\gamma = 5$ , $\Delta t = 0.01$ . . . . .	12
2	Divergence of Bénard problem: exact steady solution obtained from a multigrid program. . . . .	13
3	Convergence to steady state: solution of equation (14) showing arbitrary initial data; nine modes used ( $T_0$ to $T_8$ ), $\gamma = 3$ , $\Delta t = 0.01$ , $U = V = 1$ , $Pe = 1$ . . . . .	14
4	Convergence to steady state: solution of equation (14) with arbitrary initial data showing the function at $t = 2$ ; nine modes used ( $T_0$ to $T_8$ ), $\gamma = 3$ , $\Delta t = 0.01$ , $U = V = 1$ , $Pe = 1$ , maximum error $\leq 1 \times 10^{-4}$ . . . . .	15
5	Solution to Burgers equation at $t = 0.5$ with error $\leq 5 \times 10^{-7}$ ; 17 modes used ( $T_0$ to $T_{16}$ ), $\gamma = 5$ , $\Delta t = 0.001$ , $\alpha = 1$ , $\beta = 2$ , $\nu = 0.001$ . . . . .	16

## GENERALIZED DUFORT-FRANKEL SPECTRAL METHODS

By

Liviu Lustman\*

### ABSTRACT

This report presents an explicit time-advancing scheme for the spectral solution of parabolic equations. Several two-dimensional examples are considered, including convection-diffusion and nonlinear problems, under various boundary conditions. Numerical evidence demonstrates the efficiency and accuracy of the spectral approach.

This work was performed in collaboration with David Gottlieb, Tel Aviv University/Institute for Computer Applications in Science and Engineering.

### GENERALIZED DUFORT-FRANKEL SCHEMES

#### Introduction

Gottlieb and Gustafsson (ref. 1) presented an explicit, unconditionally stable formula for time-advancing parabolic equations, while preserving high accuracy in space. The present work treats, as a special case, the Tschebyscheff collocation spectral method as the spatial derivative approximation. Large  $\Delta\tau$  may be employed, much above the limit  $O(N^{-4})$  needed for straightforward explicit methods which use  $T_0, T_1, \dots, T_N$ . Thus the computation becomes efficient, while spectral accuracy is still maintained. Let us review the generalized Dufort-Frankel method for the simplest diffusion equation:

$$u_t = \sigma u_{xx} \tag{1}$$

The original Dufort-Frankel scheme is

---

\* Research Assistant Professor, Department of Mathematical Sciences, Old Dominion University, Norfolk, VA 23508

$$\frac{u_j^{n+1} - u_j^{n-1}}{2\Delta t} = \sigma \frac{u_{j+1}^n + u_{j-1}^n - 2u_j^n}{\Delta x^2} - \frac{\sigma}{(\Delta x)^2} (u_j^{n+1} + u_j^{n-1} - 2u_j^n) \quad (2)$$

As usual,  $u_j^n = u(j\Delta x, n\Delta t)$ . The first term on the right-hand side is the simplest approximation to  $u_{xx}(j\Delta x, n\Delta t)$ . It may be replaced by other approximations, e.g. higher order finite difference, finite element, or spectral. The second term on the right-hand side is also modified by a multiplier  $\gamma > 0$ . Large enough values of  $\gamma$  ensure unconditional stability (as proved for various cases in ref. 1).

Finally, the method we shall employ is

$$\frac{u_j^{n+1} - u_j^{n-1}}{2\Delta t} = \sigma (u_{xx})_j^n - \gamma \frac{\sigma}{\Delta x^2} (u_j^{n+1} + u_j^{n-1} - 2u_j^n) \quad (3)$$

Here  $u_j^n = u(x_j, n\Delta t)$ , where  $x_j$  ( $0 \leq j \leq N$ ) is the Tschebyscheff collocation mode;  $\Delta x$  may be taken to be  $1 - \cos \frac{\pi}{N}$  (minimal distance between nodes) or, for better accuracy:

$$\Delta x \equiv \Delta x_j = x_j - x_{j+1} \quad (4)$$

Obviously  $(u_{xx})_j^n$  is computed spectrally, and equation (3) is solved explicitly for  $u_j^{n+1}$ .

It is important to mention that equation (3) is consistent, within  $O(\Delta t^2)$ , with a wave equation:

$$\frac{1}{\sigma} u_{tt} = u_{xx} - \frac{u_{tt}}{c^2} \quad (5)$$

where the speed  $c$  is given by

$$c^2 = \left(\frac{\Delta x}{\Delta t}\right)^2 \frac{1}{\gamma} \quad (6)$$

However, equations (1) and (5) share the same steady states as  $t \rightarrow \infty$ ; also, if  $\Delta t = O(\Delta x^2)$ , equation (3) becomes consistent with equation (1) within  $O(\Delta t^2)$ .

The generalization to two dimensions:

$$u_t = \sigma_1 u_{xx} + \sigma_2 u_{xy} + \sigma_3 u_{yy} \quad (7)$$

is straightforward:

$$\frac{u_{jk}^{n+1} - u_{jk}^{n-1}}{2\Delta t} = (\sigma_1 u_{xx} + \sigma_2 u_{xy} + \sigma_3 u_{yy})_{jk}^n - \gamma \left( \frac{\sigma_1}{\Delta x_j^2} + \frac{\sigma_3}{\Delta y_k^2} \right) \cdot (u_{jk}^{n+1} + u_{jk}^{n-1} - 2u_{jk}^n) \quad (8)$$

It is also possible to replace  $\Delta x_j$  and  $\Delta y_k$  by their minimal values. Note the simplicity in the treatment of the mixed term  $u_{xy}$ .

It is convenient to define "fluxes" for equation (5) since these are the quantities actually treated by the numerical scheme:

$$u_t = \frac{\partial}{\partial x} f + \frac{\partial}{\partial y} g \quad (9)$$

with fluxes  $f$ ,  $g$ :

$$f = \sigma_1 u_x + \frac{1}{2} \sigma_2 u_y$$

$$g = \sigma_3 u_y + \frac{1}{2} \sigma_2 u_x$$

Note that there is nonuniqueness in the definition of  $f$  and  $g$ : for example, one might take

$$f = \sigma_1 u_x$$

$$g = \sigma_2 u_x + \sigma_3 u_y$$

and still end up with equation (7).

The solution is implemented as follows:

#### Algorithm

(1) The first two levels  $u_{jk}^0$ ,  $u_{jk}^1$  are stored ( $u^0$  is, of course, the initial data, but  $u^1$  must be obtained by some different method).

Set  $t = \Delta t$ ,  $n = 1$ .

(2) The fluxes are computed using  $u_{jk}^n$ .

(3) The fluxes are updated on those parts of the boundary where  $\frac{\partial u}{\partial n}$  is specified.

(4) The fluxes are differentiated to obtain the "parabolic" term

$$\frac{\partial f}{\partial x} + \frac{\partial g}{\partial y}.$$

(5)  $u_{jk}^{n+1}$  is computed from equation (6).

(6)  $u_{jk}^{n+1}$  is updated on those parts of the boundary where  $u$  is specified.

(7)  $t \leftarrow t + \Delta t$ ,  $n \leftarrow n + 1$ , go to step (2).

Note that only first-order (numerical) derivatives are required in steps (2) and (4). Thus there is one derivation routine, which is the usual straightforward  $T'_n$  formula. In certain cases, however, high mode interactions cause instabilities, and the high coefficients generated by differentiation must be smoothed. The smoothing:

$$a_k \rightarrow a_k \quad k < \frac{N}{3}$$

$$a_k \rightarrow a_k \frac{(k - N)^4}{\left(\frac{N}{3} - N\right)^4} \quad k \geq \frac{N}{3} \quad (10)$$

is then included in the derivative routine. The updating of values in step (3) varies from problem to problem. The best results have been obtained by overspecifying data, i.e. prescribing  $f$  when  $\frac{\partial u}{\partial x}$  is given. It is also possible to compute  $f$ ,  $g$  from the correct data  $\frac{\partial u}{\partial n}$ , while the tangential derivative needed is extrapolated along characteristics. Of course, the characteristics pertain to the wave equation [eq. (5)].

The analysis of reference 1 could be applied directly to equation (3) to prove stability, except for the very complicated structure of the "parabolic term" operator, which also depends on boundary conditions. For certain cases, Orszag (ref. 2) has numerically computed the eigenvalues of this operator, which turned out to be all real — a sufficient condition for stability, according to Gottlieb and Gustafsson (ref. 1).

Actual computation, as presented in the following sections, amply justifies the assumption that generalized Dufort-Frankel Tschebyscheff schemes are stable for appropriate multipliers  $\gamma$ .

### DIFFUSION EQUATIONS WITH CONSTANT COEFFICIENTS

This section summarizes results obtained for the equation

$$u_t = u_{xx} + u_{yy} + 2\epsilon u_{xy} \quad (11)$$

For parabolicity,  $|\epsilon| < 1$ . The domain considered is  $|x| \leq 1$ ,  $|y| \leq 1$ ,  $t \geq 0$ , with  $u$  specified initially and either  $u$  or  $\frac{\partial u}{\partial n}$  specified at  $|x| = 1$ ,  $|y| = 1$ .

An analytic solution has always been used to check accuracy, and also to supply initial and boundary values, as well as first level values  $u(x,y,t = \Delta t)$ . No smoothing of coefficients was done, and fluxes were overspecified on boundaries. The first check was to test whether our numerical method [eq. (10)] actually admits larger  $\Delta t$  than the obvious explicit method:

$$\frac{u_j^{n+1} - u_j^n}{\Delta t} = (u_{xx} + u_{yy} + 2\epsilon u_{xy})_j^n \quad (12)$$

A comparison, done for  $\epsilon = 0$  and Dirichlet conditions everywhere, showed that  $\Delta t$  may be easily taken to be up to 50 times larger than the stability limit of equation (12). Thus, equation (10) with  $\gamma = 5$  converges for  $\Delta t = 0.001$ ,  $N = 32$ , while the explicit method diverges at  $N = 32$ ,  $\Delta t = 0.00005$  and converges only at  $N = 32$ ,  $\Delta t = 0.00002$ .

Next the various values for the multiplier  $\gamma$  were considered. In most of these computations,  $\gamma = 4$  is the stability limit. For instance,  $N = 32$ ,  $\Delta t = 0.001$  will diverge at  $\gamma = 3$ , but will converge at  $\gamma = 5$ ;  $N = 16$ ,  $\Delta t = 0.001$  will converge at  $\gamma = 3.375$  but diverge at  $\gamma = 3.25$ . Of course, the smaller  $\gamma$ , the better the approximation; however, the error increases only slightly with  $\gamma$ .

Another test is the sensitivity of the method to the definition of  $\Delta x_j$ ,  $\Delta y_k$ . If all these quantities are taken as equal [as opposed to eq. (4)], the results are less accurate and the multiplier  $\gamma$  must be larger to

produce stability. On the other hand, the ambiguity in flux definition has no influence — even if fluxes must be updated on the boundary.

The boundary flux treatment is evidently the most complex of the questions connected with the present scheme. Overspecification produces satisfactory results. The characteristic extrapolation, i.e.,

$$u_x + \epsilon u_y = \pm \frac{1}{c} u_t \quad \text{at } x = \pm 1 \quad (13)$$

seems to be less accurate. Here an analytic result would be extremely useful.

#### CONNECTION-DIFFUSION PROBLEMS

In this section the following two cases are considered:

(1) Constant coefficient problem:

$$\phi_t + U\phi_x + V\phi_y = \frac{1}{Pe} (\phi_{xx} + \phi_{yy})$$

$$0 \leq x, y \leq \pi, \quad t \geq 0$$

$\phi$  given on  $y = 0, \pi$

$\phi_x = 0$  on  $x = 0, \pi$

$\phi$  given at  $t = 0$

(14)

(2) Temperature distribution in a Bénard cell:

$$\phi_t + U(x,y)\phi_x + V(x,y)\phi_y = \frac{1}{Pe} (\phi_{xx} + \phi_{yy})$$

$$0 \leq x, y \leq \pi, \quad t \geq 0$$

$\phi = 0$  on  $y = 0$ ,  $\phi = 1$  on  $y = \pi$

$\phi_x = 0$  on  $x = 0, \pi$

$\phi(x, y, t = 0)$  given

(15)

The speeds  $U(x, y)$ ,  $V(x, y)$  representing a vortical flow are prescribed:

$$U(x, y) = -\cos y \sin x$$

$$V(x, y) = \sin y \cos x \quad (16)$$

The quantity  $Pe$  is the Péclet number of the problem:  $Pe = \frac{\text{typical speed} \times \text{typical length}}{\text{conductivity}}$ . In both cases, the fluxes have been specified as

$$\begin{aligned} f &= \frac{1}{Pe} \phi_x - U\phi \\ g &= \frac{1}{Pe} \phi_y - V\phi \end{aligned} \quad (17)$$

which is appropriate even for variable coefficients, since  $(U,V)$  is divergence free. The flux  $f_{Bd} \equiv -U\phi$  was prescribed on the boundary carrying Neumann conditions. Initial conditions have been generated arbitrarily for both equations (14) and (15), and the convergence to a steady solution was tested.

For the constant-coefficients case, an analytic solution is easily obtained which is used as before to supply boundary conditions and verify accuracy. For instance, one may take

$$\phi = \left( \cos x - \frac{UPe}{2} \sin x \right) \sinh \left( y \sqrt{\frac{(U^2 + V^2)Pe}{4} - 1} \right) e^{Pe \left( \frac{xU}{2} + \frac{yV}{2} \right)} \quad (18)$$

as a steady solution of equation (14). Formula (18) clearly shows the rapid variation of  $\phi$  with  $y$  as  $Pe$  increases. Indeed, at  $U=V=1$ ,  $Pe \approx 5$ , the computational results became quite poor, since the few modes used ( $T_0, T_1 \dots T_8$  or eventually  $T_0, T_1 \dots T_{16}$ ) could not properly resolve  $\phi \approx e^{3.5y}$ . For smaller  $Pe$  (larger conductivity), very accurate results were readily produced.

For equation (15) collocation was used to deal with the variable coefficients. It appears that enough high modes were generated to distort the solution. Some plots even show minima and maxima (there should be none inside the domain) at the nodal points. The smoothing formula [eq. (10)] provides a simple remedy to this unwanted phenomenon. For  $Pe = 10$ ,  $N = 16$  successful computations have been performed, with results in complete agreement with numerical data obtained otherwise. (There are no analytic solutions for this case). Note that the Péclet number seems higher, but, in fact, because  $U, V$  vary inside the domain, the boundary layers of equation (15) are less abrupt than those of equation (14) and resolution is easier. Using polynomials of higher degree (say 64), one could treat even higher Péclet numbers. (See also figures 1 and 2).

The convergence to the steady state is quite rapid, as seen in figures 3 and 4. Analytic solutions of equation (14), say, with homogenous conditions, decay at least as fast as

$$e^{-\left[2 + \frac{(U^2 + V^2)Pe}{4}\right]t}$$

Thus, one may use time-dependent equations — or even artificially time dependent equations — to solve steady-state convection-diffusion problems efficiently.

### BURGERS EQUATION

This is an experiment in treating nonlinear equations. The problem to be solved is

$$u_t + uu_s = \nu \frac{\partial^2 u}{\partial s^2} \quad (19)$$

where  $s$  is defined by

$$s = \frac{\alpha x + \beta y}{\sqrt{\alpha^2 + \beta^2}}; \alpha, \beta \text{ constants.} \quad (20)$$

Of course, equation (19) is rewritten as an equation in  $(x,y,t)$  domain, with boundary and initial conditions. However, these are specified in such a way as to agree with equation (19). Specifically, we solve

$$\begin{aligned} u_t + u(\alpha u_x + \beta u_y) &= \nu(\alpha^2 u_{xx} + \beta^2 u_{yy} + 2\alpha\beta u_{xy}) \\ -1 &\leq x, y \leq 1, t \geq 0 \\ u(x, y, t = 0) &= u_0(s) \\ u|_{\text{boundary}} &= u_0(s|_{\text{boundary}}, t) \end{aligned} \quad (21)$$

The fluxes are defined as

$$\begin{aligned} f &= \nu(\alpha^2 u_x + \alpha\beta u_y) - \frac{\alpha}{2} u^2 \\ g &= \nu(\alpha\beta u_x + \beta^2 u_y) - \frac{\beta}{2} u^2 \end{aligned} \quad (22)$$

This problem has been selected because of its explicit solutions, which enable comparison with the numerical results. Satisfactory convergence is again easily obtained. An example is presented in figure 5. An interesting point is that equation (21), although nonlinear, shows better

results when no smoothing is applied to the high coefficients (cf. ref. 4). This is probably due to the fact that there is enough viscosity in the equation itself.

As an example, consider

$$u(x,y,t) = \frac{0.24 \sin(1.2s)e^{-0.144t}}{0.1 + \cos(1.2s)e^{-0.144t}}$$

which is a solution of equation (19) with  $\alpha = 0.7$ ,  $\beta = 0.8$ ,  $\nu = 0.1$ . At time  $t = 0$ , the maximum value of  $u$  is  $\approx 3$  while the average value of  $u$  over  $-1 \leq x, y \leq 1$  is  $\approx 0.2$ . Thus there are steep boundary layers to be resolved. If the smoothing [eq. (10)] is applied, the result is much too damped; without smoothing, for  $N = 16$ ,  $\gamma = 15$ , an error of about  $5 \cdot 10^{-4}$  is maintained for  $0 < t < 0.5$ , corresponding to 500 steps ( $\Delta t = 0.001$ ).

#### DISCUSSION

The purpose of this research program was to obtain better time increments than those allowed by the naive scheme [eq. (12)], while retaining the desirable spectral accuracy. Here other possible solutions to this problem will be briefly described. One is presented in reference 5, where the explicit time-stepping operator is modified in such a way as to make it bounded for all  $\Delta t$ . This method is efficient for Fourier expansions, but not for Tschebyscheff expansions. After some experimentation it was found that the modified operator, while stable, differs too much from the exact one, and the approximations are inconsistent.

Another method is to employ approximate inverses (ref. 2). These are operators, simple in structure, which approach the spectral ones. Implicit time stepping is used, with arbitrary  $\Delta t$ , and the inversions needed are performed on the simpler operators. To make the procedure efficient in multidimensions, some type of splitting must be used, introducing problematic boundary treatment. Mixed terms also pose problems (ref. 6) compared with the simplicity of equation (8). Yet another possibility is to generalize Saulev's scheme (ref. 7) to spectral methods in the same way equation (2) is generalized to equation (3). This seems a very promising perspective, and a probable direction for future work.

## CONCLUSIONS

A simple and efficient time-advancing scheme has been presented for spectrally solving parabolic equations with general boundary conditions. Various equations have been used, obtaining satisfactory results, especially for convergence to steady states and Dirichlet boundary conditions.

While the main theoretical question — stability — is still open, these preliminary results provide a firm foundation for further research.

## REFERENCES

1. Gottlieb D.; and Gustafsson, B.: Generalized Dufort-Frankel Methods for Parabolic Initial-Boundary Value Problems. SIAM J. Numer. Anal., Vol. 13, 1976, p. 129.
2. Orszag, S.A.: Spectral Methods for Problems in Complex Geometry. Spectral Methods for Problems in Complex Geometry. J. Comp. Phys., Vol. 37, 1980, p. 70.
3. Engquist, B.; and Majda, A.: Absorbing Boundary Conditions for the Numerical Simulation of Waves. Math. Comp., Vol. 31, 1977, p. 629.
4. Gottlieb, D.; Lustman, L.; and Orszag, S.A.: Spectral Calculations of One Dimensional Inviscid Compressible Flow. ICASE Report 80-34, 1980.
5. Gottlieb, D.; and Turkel, E.: On Time Discretizations for Spectral Methods. To appear in Studies in Appl. Math.
6. Lustman, L: Spectral Methods in Compressible Flow Problems. Progress Report for NASA Grant NAG-1-25, Feb. 1981.
7. Richtmyer, R.D.; and Morton, K.W.: Difference Methods for Initial Value Problems. 2nd Edition, John Wiley & Sons, 1967.

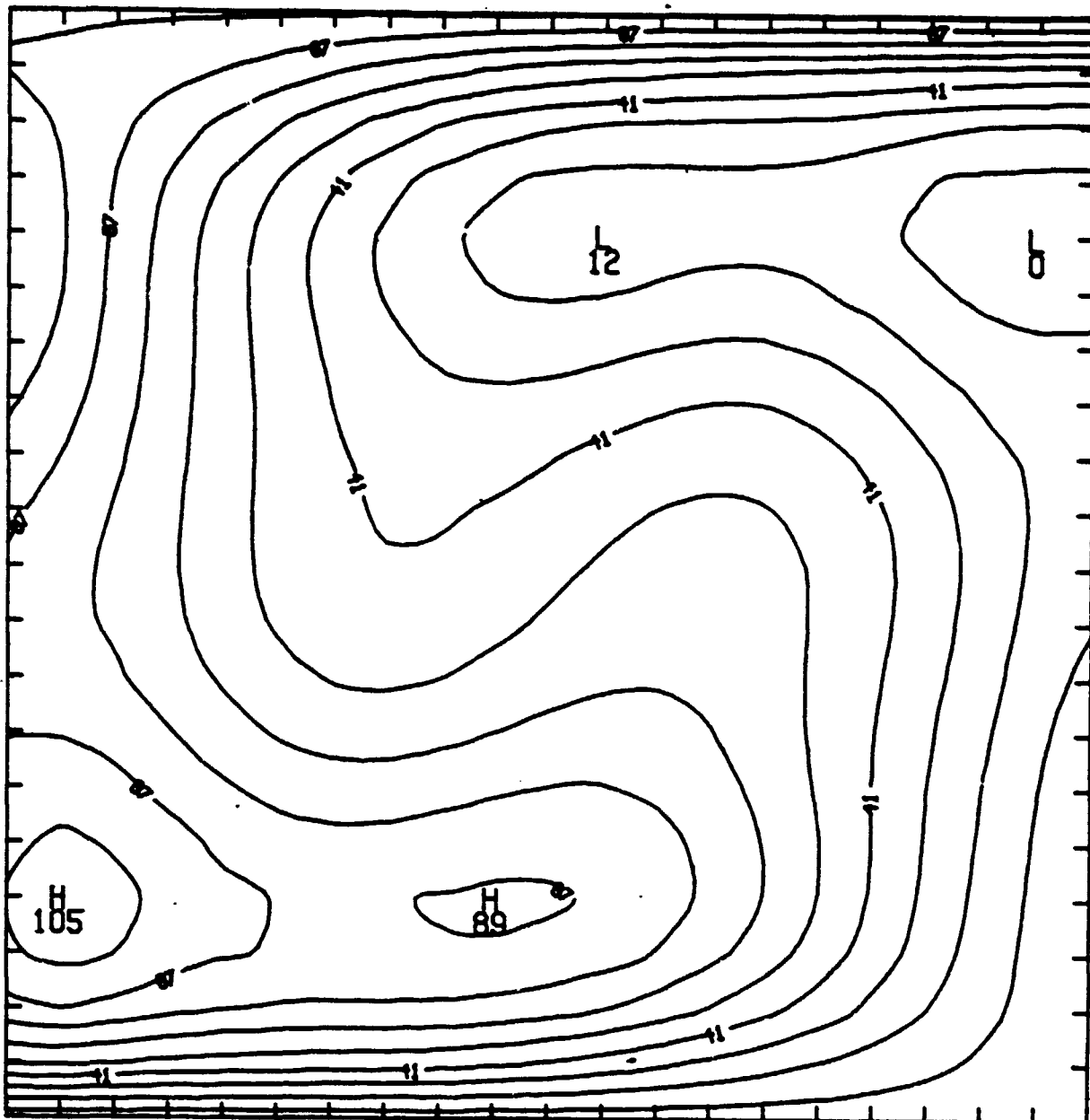


Figure 1. Divergence of Bénard problem at  $Pe = 50$  showing lines of constant  $\phi$  at  $t = 4$ , computed using nine modes ( $T_0$  to  $T_8$ ),  $\gamma = 5$ ,  $\Delta t = 0.01$ .

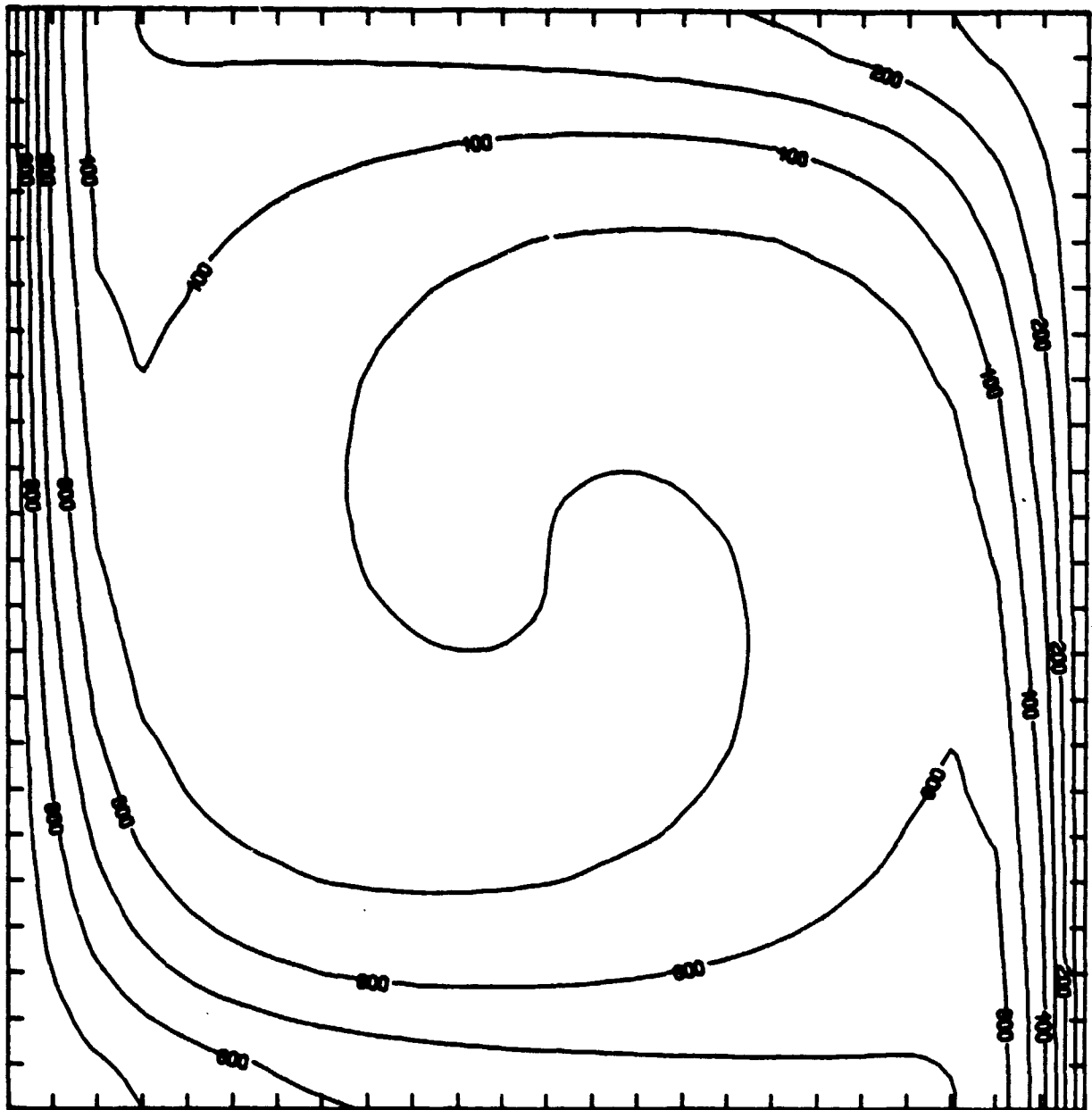


Figure 2. Divergence of Bénard problem: exact steady solution obtained from a multigrid program. (The x and y axes are interchanged with respect to figure 1.)

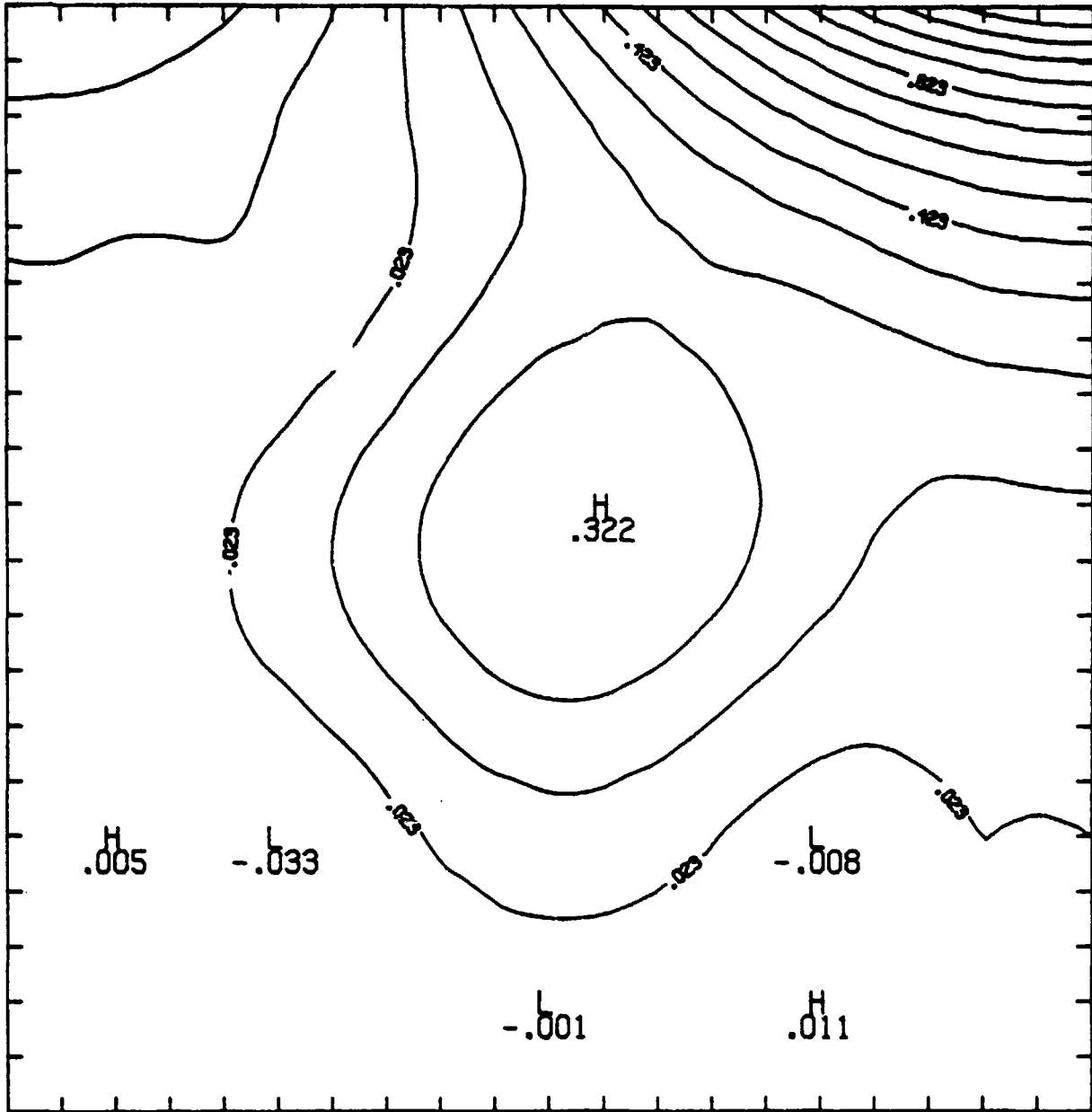


Figure 3. Convergence to steady state: solution of equation (14) showing arbitrary initial data; nine modes used ( $T_0$  to  $T_8$ ),  $\gamma = 3$ ,  $\Delta t = 0.01$ ,  $U = V = 1$ ,  $Pe = 1$ .

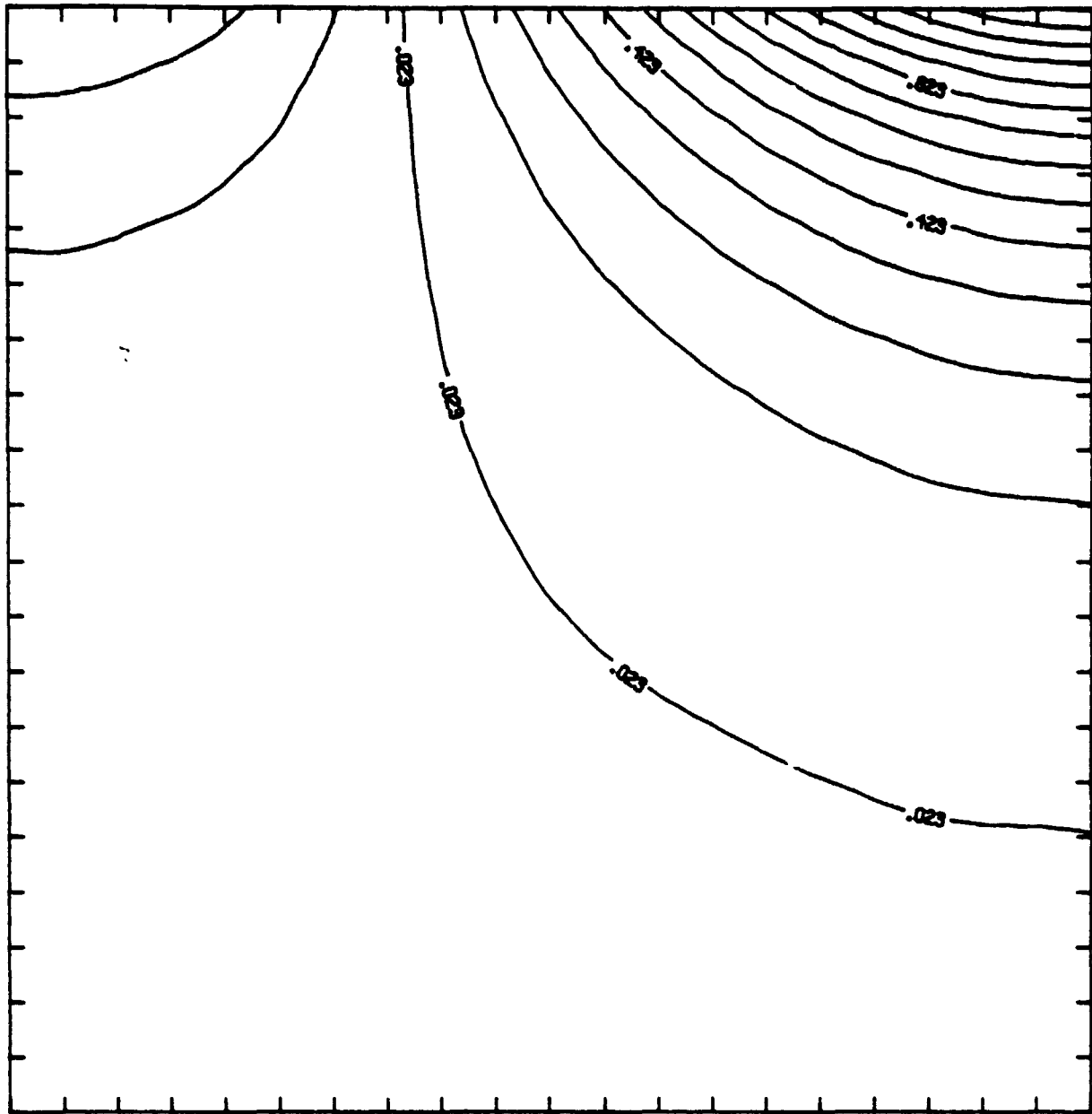


Figure 4. Convergence to steady state: solution of equation (14) with arbitrary initial data showing the function at  $t = 2$ ; nine modes used ( $T_0$  to  $T_8$ ),  $\gamma = 3$ ,  $\Delta t = 0.01$ ,  $U = V = 1$ ,  $Pe = 1$ , maximum error  $\leq 1 \times 10^{-4}$ .

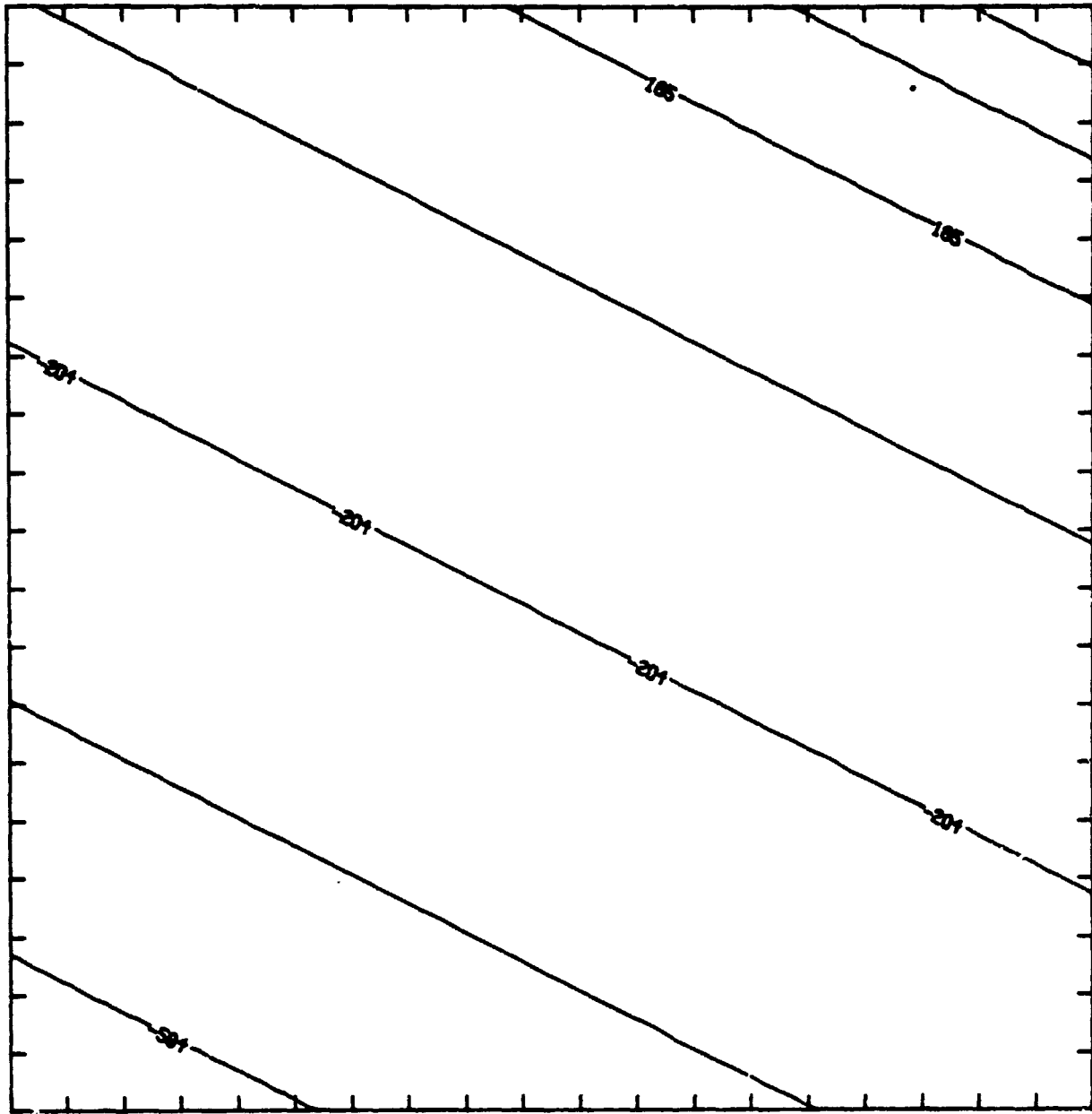


Figure 5. Solution to Burgers equation at  $t = 0.5$  with error  $\leq 5 \times 10^{-7}$ ; 17 modes used ( $T_0$  to  $T_{16}$ ),  $\gamma = 5$ ,  $\Delta t = 0.001$ ,  $\alpha = 1$ ,  $\beta = 2$ ,  $\bar{v} = 0.001$ . Note that although equation (21) is written in terms of  $x$  and  $y$ , the solution  $u = \text{constant}$  on lines  $s = \text{constant}$  (straight lines of slope - 1:2).